SEMARAK ILMU
PUBLISHING

Journal of Advanced Research in Fluid Mechanics and Thermal Sciences

Journal homepage:
https://semarakilmu.com.my/journals/index.php/fluid_mechanics_thermal_sciences/index
ISSN: 2289-7879

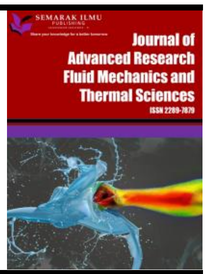

Numerical Analysis of the Phase Change Material Impact on the Functionality of a Hybrid Photovoltaic Thermal Solar System in Transient Conditions

Mohamed Bouzelmad[1,*], Youssef Belkassmi[1,*], A. S. Abdelrazik[2], Abdelhadi Kotri[3], Mohammed Gounzari[1], Mustapha Sahal[1]

[1] Laboratory of Physics, Energy and Information Processing (Lab.PETI), Polydisciplinary Faculty of Ouarzazate, University Ibn Zohr, Agadir, Morocco
[2] Interdisciplinary Research Center for Sustainable Energy Systems (IRC-SES), King Fahd University of Petroleum & Minerals, 31261, Dhahran, Saudi Arabia
[3] ESEF, University of Chouaib Doukkali, El Jadida, Morocco

ARTICLE INFO

Article history:
Received 22 August 2023
Received in revised form 5 November 2023
Accepted 18 November 2023
Available online 15 December 2023

Keywords:
Photovoltaic thermal system; phase change material; performance assessment

ABSTRACT

Combining phase change material with a hybrid photovoltaic thermal system can be a reasonable solution for excessive temperature distributions and inadequate heat control in traditional photovoltaic thermal modules. This work proposes a mathematical model to assess the transient processes of a hybrid photovoltaic thermal solar system with phase change materials in comparison to a conventional photovoltaic panel. The studied hybrid module is composed of (the cover glass, photovoltaic plate, absorber plate, phase transition materials layer, and water in the tubing). The employed system parameters were selected on an energy-saving basis in the different system layers. The differential equations determining energy exchange between the different parts in both systems were numerically solved using the Finite Difference Method applied to MATLAB software. The transient model's validity is first tested by comparing the prediction temperatures of each layer of the photovoltaic thermal system with those numerical and experimental studies in literature in which the maximum discrepancy is less than 1.5°C. Then, the results of the transient model are investigated in real outdoor weather conditions using meteorological data. The results illustrated that the hybrid module diminishes the temperature of the photovoltaic layer by roughly 21.9°C compared to the standalone photovoltaic panel, leading to a 1.95 % enhancement in electrical performance.

1. Introduction

Using traditional energy sources to satisfy domestic and industrial needs is often costly, polluting, and exhaustible [1]. To remedy these problems, the use and research of alternative energy resources are essential [2]. Renewable energies, particularly solar energy, are one of the most potential fields and represent an encouraging solution, more and more used nowadays, present everywhere, and

* *Corresponding author.*
E-mail address: mohamed.bouzelmad@edu.uiz.ac.ma

https://doi.org/10.37934/arfmts.112.1.121

practically inexhaustible. A part of the incident solar radiation on a PV panel is transformed into continuous electrical energy via the PV cells; the remainder of the unconverted energy heated the PV cells, raising their operating temperature and decreasing electrical energy output [3].

The temperature of PV cells diminishes when the photovoltaic panel is combined with the thermal system, which enables a hybrid photovoltaic system to absorb heat [4,5]. In this regard, researchers have recovered several techniques for improving the electrical conversion efficiency of a standard PV panel. Autonomous PV collectors with phase change material (PCM) thermal energy storage have additionally been investigated in a few works of literature [6]. According to the literature, the PV/Thermal (PV/T) system is fascinating. It has a bright future as the amount of energy generated by renewable energy sources grows annually, and this technology should be used in various applications [7-9]. Today's PV implementation exceeds 500 GW, and the average sale price remains low, reaching 0.26 $ per watt in July 2018, depending on the crystalline silicon solar cells that are the first materials to be developed and the most extensively utilized, representing nearly 90 % of the market [10,11].

Additionally, several previous studies have investigated the incorporation of PCMs in PV/T systems [10-18]. Indeed, reducing the temperature of PV cells using PCM was highly recommended as it does not require additional energy or function [19]. Furthermore, the PCM was reported to be used for PV cooling; however, it must have specific properties, namely elevated latent heat of fusion, greater thermal conductivity, non-corrosive, low non-toxicity, a melting temperature within the operating temperature of the PV module, minimal sub-cooling, and to be chemically stable [20]. It should be noted that the latest research on passive cooling of PV modules, namely the use of PCMs, has revealed that PCMs could stock a significant value of thermal energy, which kept the temperature of PV panels almost constant.

Numerous scientific investigations have proposed different designs for hybrid PV-based modules. Early in the last decade, Hasan *et al.,* [21] experimentally studied the cooling of PV cells using PCM and reported that the PV module with the PCM had higher effectiveness than the standalone PV. They concluded that the PV system incorporating the PCM was more efficient than the conventional one because of the cells' reduced temperature. Hussain *et al.,* [22] have studied the effectiveness of employing a heat exchanger made of aluminum honeycomb in the backside of the PV to improve the thermal effectiveness of an air-cooled PV/T hybrid collector. It was found that the performance under various flow rates. At an air mass flow rate of 0.11 kg/s, introducing honeycomb channels enhanced the thermal effectiveness from 27% to 87% because air usage for cooling had limited thermophysical properties. The improvement in electrical efficiency was essentially limited (0.1%). According to studies on electricity production and performance conducted by Park *et al.,* [23], the range of electric power produced by the photovoltaic panel was improved by 1.0 -1.5% compared to conventional PV panels. Besides, the PV/PCM system performance was improved by roughly 3.1%.

In the same context, Fudholi *et al.,* [24] have studied various water-cooled PV/T configurations at various mass flow rates and solar radiation values. They have proposed three innovative absorber pipe models: band diffusion accumulator, spiral heat transfer absorber, and direct flow collector. The PV temperature reduced as the mass flow rate rose, and the electrical performance enhanced. In addition, raising the quantity of sunlight improved the temperature of the PV panels and the produced electrical effectiveness. They indicated the comparison of the actions of the spiral flow absorbers and direct flow; directly absorbing the flow had greater thermal effectiveness, whereas the coiled stream absorber has maximum electrical effectiveness at incident sunlight of 800 W/m^2, the coiled stream absorber had the best global effectiveness, with electrical, thermal, and total efficiencies of 13.8 %, 54.6%, and 68.4 %, respectively. Hou *et al.,* [25] have also created a method based on a small heat pipe network. To examine the new PV/T, a numerical study with the new heat pipe network was developed. It has been reported that where the supply water temperature in the two situations was at the surrounding temperature, the thermal effectiveness of the new system, according to the seasonal temperature, dropped to under 20% in winter and achieved roughly 40% in summer.

In 2019, Huo *et al.,* [26] introduced a new hybrid PV/T system. They concurrently adopted the pipe sunlight layer detector to transform solar radiation into electricity and thermal energy. The authors found that the module's temperature was diminished by 3.5 to 6.5 °C. They also discovered that the electrical efficiency was enhanced by 13.7 to 25.3 %. The thermal efficiency was also increased from 7.6% to 10.7%. The global efficiency of the system was enhanced from 8.7% to 12.7%. The same year, Abdelrazik *et al.,* [27] numerically investigated the hybrid PV/T systems with a layer of nano-enhanced PCM (nanoPCM) introduced between the PV and thermal layers. According to their reports, the PV/T-PCM and the nanoPCM systems have a maximum electrical efficiency enhancement of 1.7 and 2.7 % compared to the PV conventional system, respectively.

On the other side of the studies, the high potential of nanofluids attracted the interest of numerous investigators in several ways [28]. For instance, Samylingam *et al.,* [29], in 2020, used MXene nanoparticles (Ti_3C_2) hanging in pure olein palm oil (OPO). They have evaluated the thermal and energy effectiveness of a PV/T hybrid solar thermal module. They have found an enhancement of heat transfer coefficient of 9 % was reached compared to PV/T with Al2O3-water when the Mxene nanofluid was used. The MXene-based nanofluid reduced the PV temperature by 40% compared to the conventional PV panel.

In 2021, Das *et al.,* [30] experimentally investigated a new rectangular coiled pipe absorber design using a translucent multi-crystalline PV panel and absorber pipes attached to the back of the PV. Utilizing PCM (OM35) and biochar generated from water hyacinth, a new shape-stable composite was developed using a simple impregnation approach. Because of its blackish look, this novel composite was also integrated into the envelope of the PV panel and the rear cover to increase cooling homogeneity and improve absorption of incident sunlight. It was discovered that the PV/T system temperature could be reduced by 29% compared to the PV system, electrical energy output could be increased by around 18.4 %, and system thermal efficiency might be increased from 60.3% to 71.2%. The new PCM-biochar component was able to stabilize the highest operating temperatures of the PV/T system within a secure range and enhance the life of the system. In the same period, Ke *et al.,* [31] proposed numerical and experimental investigations to study the electrical and thermal performance of air-cooled PV/T systems with PCMs. The research was conducted during 4 Hefei weather conditions and with two PCM sheets of air channel solar chimney. The findings revealed that the presence of PCM aided in regulating the inside thermal surroundings. The PCM varies played a vital role in PCM effectiveness over 4 days in winter when the PCM range is 19-21 °C.

Recently, Abdelrazik *et al.,* [32] have investigated six configurations of the hybrid PV-based systems that encountered different combinations of optical filtration (OF) channel, cooling fluid (CF) channel, and nanoPCM layer. The systems were the conventional PV, besides the hybrid OF/PV, PV/CF, OF/PV/CF, PV/nanoPCM/CF, and OF/PV/nanoPCM/CF systems. The results revealed that optical filtration (OF), coupled with coolant (CF), emerged as among the most effective methods to cool PV. It achieved a 42.1% and 6.3 % reduction compared to the average PV temperature of traditional PV and PV/T modules. Additionally, OF existence reduced the drawback of low nanoPCM thermal conductivity with lower regulated temperature distribution.

The literature reveals that the numerical investigation of PV/T-PCM modules has already been the subject of limited research. This research has focused mainly on improving system productivity by increasing the cooling of PV modules utilizing PV/T-PCM systems. To the authors' knowledge, no numerical studies have been carried out on utilizing RT30 as PCM integrated with the hybrid PV/T system. Besides, there were no investigations on the numerical analysis of the transient model of this kind of system using actual input data to study the effect of several parameters such as incident irradiation, ambient temperature, and wind speed as meteorological input data on the temperature variation in the PV/T-PCM system.

This work uses a computational approach to assess the transient processes of a hybrid PV/T solar system with phase change materials (PV/T-PCM). Comparisons are reported between the hybrid PV/T-PCM system from one side and the conventional standalone PV and hybrid PV/T systems from the other. The impact of latent cooling on the standalone PV module was also investigated. The performance enhancements, in terms of electrical yield and temperature achieved by PV/T and PV/T-PCM, are compared with a standalone PV module and then discussed against literature reports. The actual weather of Ouarzazate (Latitude: 30°91'N, Longitude: − 6°89' W) city-Morocco over two days, one day in summer and one day in winter, are examined.

2. Methodology

2.1 Structure of the PV/T-PCM Module

The principal parts of the PV/T-PCM module are the PV panel and the solar collector. PV cell comprises monocrystalline silicon cells with an optimal transformation efficiency of 20 %. Table 1 summarizes the PV module's performance data. The PV/T-PCM systems with the plate and tube form offer lower water capacity needs, overall pressure-bearing potential, and more building flexibility. The glazing is part of the PV/T-PCM model employed in this work, which includes the thermal absorber, PCM layer, insulation, pipe, and cooling water.

Figure 1 exhibits the front view of the system PV/T_PCM. An air gap separated the top glazing from the PV plate. Below the PV panel, eight tubes made of copper were linked to the underside of the copper absorber plate. The side and bottom surfaces of the PV/T-PCM solar collector were covered with a white glass wool thermal insulation layer. The water entry and exit ends were installed at the bottom cross tubes (see Figure 1).

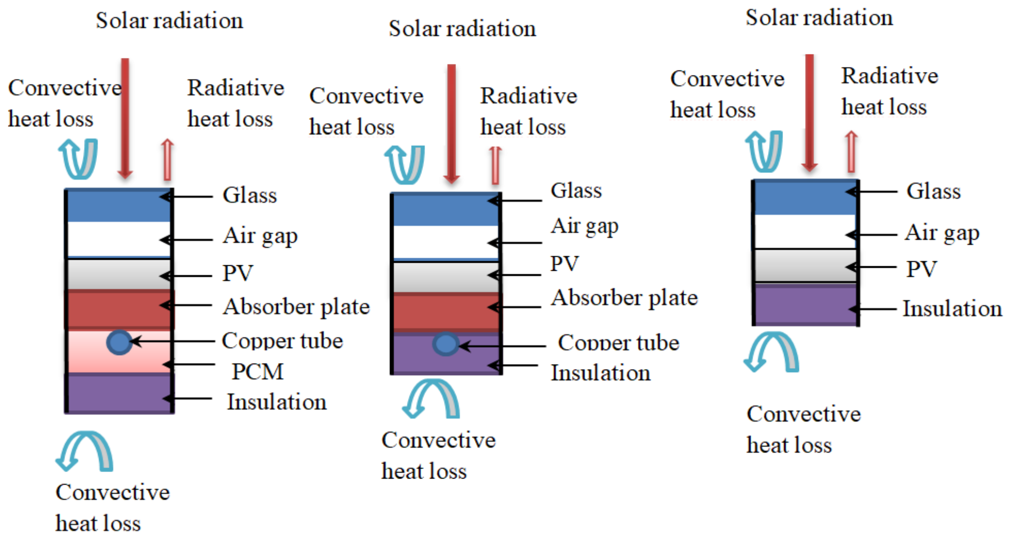

(a) (b) (c)

Fig. 1. The design of the front view of the (a) PV/T-PCM, (b) PV/T system, and (c) standalone PV system

2.2 Mathematical Model

The proposed approach is split up into height vertices perpendicular to the direction of liquid flow (see Figure 1): crystal covering, air chasm, PV cell, absorber, fluid, PCM, and insulation. In addition, the equations governing the temperatures T_g, T_a, T_{pv}, T_{ab}, T_t, T_f, T_{pc}, and T_i were developed using the energy balance of one-dimensional heat transfer Eq. (1) as given by Faddouli *et al.,* [33]. Furthermore, three distinct heat transfer processes are expected: convection, conduction, and radiation, as shown in Figure 1. The computer application was created using MATLAB software. Moreover, the rising temperatures of every hybrid photovoltaic network element were estimated by dividing the temperature field of each layer along the respective wall.

$$\frac{dE}{dt} = q_{in} + q_u - q_{ou} \tag{1}$$

Here, dE/dt, q_{in}, q_u, and q_{ou} denote the energy variation of the internal system, the rate of heat transfer into the system, the amount of heat production in the model, and the heat transfer rate out of the system, respectively.

a. Glass cover

The cover is thin, sufficient to allow the element's characteristics to be assumed steady and the temperature uniform. Heat transfer in glass is generally triggered by the irradiation of the sun and the absorber and the convection between the glass, nature, and the air gap (Eq. (2)).

$$\rho_g c_g \delta_g \frac{\partial T_g}{\partial t} = \left(\alpha_g G\right) + h_{cv,g-am}\left(T_{am} - T_g\right) + h_{cv,g-a}\left(T_a - T_g\right) + h_{r,g-pv}\left(T_{pv} - T_g\right) \tag{2}$$

G and α_g denote the incident radiation and the absorptivity of the glass protect, respectively. A similar heat transfer coefficient for the front of the glass shield is given in Eq. (3) as given by Faddouli *et al.,* [33].

Eq. (4) and Eq. (5) also express the transfer coefficients between the PV module, the glass cover, and the air, respectively.

$$h_{cv,g-am} = \frac{\sigma \varepsilon_g (T_g^4 + T_{sky}^4)}{T_g - T_{am}} + \frac{Nu_{am} \lambda_{am}}{\delta} \tag{3}$$

$$h_{r,g-pv} = \frac{\sigma (T_{pv}^2 + T_g^2)(T_{pv} + T_g)}{\frac{1}{\varepsilon_{pv}} + \frac{1}{\varepsilon_g} - 1} \tag{4}$$

$$h_{cv,g-a} = \frac{Nu_a \times \lambda_a}{\delta_a} \tag{5}$$

The above equation T_{sky} denotes the sky temperature whose value ($0.0552.T_{am}^{1.5}$) is given by Swinbank [34]. It is noted that the convective heat exchange coefficient ($h_{cv,g-a}$) between the PV panel and the underside area of the glass is indicated as a relation to the distance differentiating the glass cover and the PV panel δ_a, (see Eq. (6)) and the Nusselt number (see Eq. (7)).

$$Nu_{am} = 0.86\,\mathrm{Re}_{am}^{\frac{1}{2}}.\mathrm{Pr}_{am}^{\frac{1}{3}} \tag{6}$$

$$\delta = \frac{4.a.b}{\sqrt{a^2+b^2}} \tag{7}$$

where Pr, Re, a, and b denote the Prandtl number, the Reynolds number, the panel length, and the width, respectively. The radiation transfer coefficient in both the absorber and the glass cover is given by Duffie *et al.,* [35]. The Nusselt number (Eq. (8)) is given by Hollands's formula [36].

$$Nu_a = 1+1.44\left[1-\frac{1708\left(\sin(1.8\times\theta)\right)^{1.6}}{Ra.\cos(\theta)}\right]\times\left[1-\frac{1708}{Ra.\cos(\theta)}\right]^{+}+\left[\left(\frac{Ra.\cos(\theta)}{5830}\right)^{\frac{1}{3}}-1\right]^{+} \tag{8}$$

The symbol $[]^{+}$ used in Eq. (8) signifies that if the amount in parentheses is negative, it must reset to zero. Eq. (9) gives the Rayleigh number.

$$Ra = \frac{g.\beta(T_{pv}-T_g)\delta_a^3}{\nu_a.k_a} \tag{9}$$

where δ_a, k_a ,ν_a, and β the characteristic width (length between the glass cover and the absorber), the thermal conductivity, the dynamic viscosity, and the thermal expansion coefficient, respectively [37].

b. Air gap

Convection transfers heat inside this area between the PV cell in the lower section and the air gap and the cover on the top side, assuming that the thermophysical characteristics of the air are in a transient state (Eq. (10)). Additionally, the convective heat coefficient is expressed as $h_{cv,\mathrm{a}-pv} = h_{cv,\mathrm{a}-g} = Nu_a.\lambda_a / \delta_a$.

$$\rho_a c_a \delta_a \frac{\partial T_a}{\partial t} = h_{cv,\mathrm{a}-g}(\mathrm{T}_g - \mathrm{T}_a) + h_{cv,\mathrm{a}-pv}(T_{pv}-T_a) \tag{10}$$

c. The PV module

The heat transfer equation of the PV module is written as follows in Eq. (11) as given by [38]:

$$\rho_{pv} c_{pv} \delta_{pv} \frac{\partial T_{pv}}{\partial t} = \left(\tau_g \alpha_{pv}\,\mathrm{G}\right) + h_{cv,pv-a}(T_a - T_{pv}) + \mathrm{h}_{\mathrm{r},pv-g}(T_g - T_{pv}) + h_{cd,pv-ab}(T_{ab}-T_{pv}) - q_u \tag{11}$$

While $h_{cv,pv-a}$, $h_{r,pv-g}$, and $h_{cd,pv-ab}$ denote the coefficient in terms of heat exchange via convection between the photovoltaic sheet and air gap, the coefficient of the heat exchange via irradiation from glass cover to PV sheet and the coefficient of the heat exchange via conduction between the PV cell and absorber, respectively. These coefficients are given by Eq. (12) to Eq. (14).

$$h_{cv,a-pv} = h_{cv,pv-a} \tag{12}$$

$$h_{r,pv-g} = h_{r,g-pv} \tag{13}$$

$$h_{cd,pv-ab} = \frac{\lambda_{ab}}{\delta_{ab}} \tag{14}$$

The electrical energy q_u used in Eq. (11), can be computed using Eq. (15):

$$q_u = \eta_{el}.\mathrm{P.G} \tag{15}$$

Where P, G, and η_{el} denote the packing factor, the irradiation, and the electrical efficiency of the solar cell (see Eq. (16)), respectively. Furthermore, in this work, it was supposed that the network performs under transient state conditions. Therefore, the electrical efficiency of the PV model, which relies on the reference cell efficiency (η_{ref}) at a reference operating temperature (T_{ref}) and temperature coefficient (β_{pv}), is expressed using the formulas reported by Bhattarai *et al.,* [39].

$$\eta_{el} = \eta_{ref}[1-\beta_{pv}(T_{pv}-T_{ref})] \tag{16}$$

d. The absorber

The equation governing the heat transfers for the absorber layer is given by Eq. (17).

$$\rho_{ab}c_{ab}\delta_{ab}\frac{\partial T_{ab}}{\partial t} = h_{cd,pc-ab}(\mathrm{T}_{pc}-\mathrm{T}_{ab}) + h_{cd,pv-ab}(\mathrm{T}_{pv}-\mathrm{T}_{ab}) + h_{cd,ab-t}(T_t - T_{ab}) \tag{17}$$

The heat coefficient of conduction and convection used in Eq. (17) was expressed as follows in Eq. (18):

$$h_{cd,pv-ab} = h_{cd,ab-pv}, h_{cd,pc-ab} = \lambda_{pc}/\delta_{pc}, h_{cd,ab-t} = \lambda_t/(d_{out}-d_{in}) \tag{18}$$

e. Tube

The equation that governs heat transfers at the tube level is expressed in Eq. (19).

$$\rho_t c_t \delta_t \frac{\partial T_t}{\partial t} = h_{cd,pc-t}(\mathrm{T}_{pc}-\mathrm{T}_t) + h_{cd,ab-t}(\mathrm{T}_{ab}-\mathrm{T}_t) + h_{cv,t-f}(T_f - T_t) \tag{19}$$

where the coefficient of conduction is $h_{cd,pc-t} = \lambda_{pc} / \delta_{pc}$, $h_{cd,ab-t} = \lambda_{ab} / \delta_{ab}$ and the coefficient of convection is $h_{cv,t-f} = (Nu_f \lambda_f) / d_{in}$.

f. PCM layer

The PCM saves the transmitted heat energy from the absorber plate. The PCM is divided into the first layer just below the absorber, the middle layers, and the last layer above the insulation governed by the energy balance Eq. (20) to Eq. (22), respectively.

$$c_{pc}.\rho_{pc}.\delta_{pc}\frac{\partial T_{pc}}{\partial t} = h_{cd,pc-ab}(\mathrm{T}_{ab} - \mathrm{T}_{s,pc}) + h_{cd,(pc,s)-(pc,l)}(\mathrm{T}_{s,pc} - \mathrm{T}_{l,pc}) + h_{cd,pc-t}(T_t - T_{pc}) \tag{20}$$

$$c_{pc}\rho_{pc}\delta_{pc}\frac{\partial T_{pc}}{\partial t} = \int_{-x}^{+x}\lambda_{pc}\frac{\partial T_{pc}}{\partial x} \tag{21}$$

$$c_{pc}\rho_{pc}\delta_{pc}\frac{\partial T_{pc}}{\partial t} = h_{cd,pc-i}(\mathrm{T}_i - \mathrm{T}_{pc}) + h_{cd,(pc,s)-(pc,m)}(\mathrm{T}_{pc,s} - \mathrm{T}_{pc,m}) \tag{22}$$

The heat transfer coefficients are given as: $h_{cd,pc-ab} = \lambda_{ab} / \delta_{ab}$, $h_{cd,pc-t} = \lambda_t / (d_{out} - d_{in})$, $h_{cd,pc-i} = \lambda_i / \delta_i$ and $h_{cd,(pc,s)-(pc,m)} = h_{cd,(pc,s)-(pc,l)} = \lambda_{pc} / \delta_{pc}$ according to the formulas developed by Atkin and Farid [19]. The heat capacity of the base PCM was determined as depicted in Eq. (23):

$$c_{pc} = \begin{cases} c_{s,pc} & T_{pc} \le T_s \\ \dfrac{4.Lh_{pc} - 4C_{s,pc}\left(T_l - T_s\right)}{\left(T_l - T_s\right)^2}\left(T_{pc} - T_s\right) + c_{s,pc} & T_s < T_{pc} \le T_m \\ \dfrac{4.Lh_{pc} - 4C_{l,pc}\left(T_l - T_s\right)}{\left(T_l - T_s\right)^2}\left(T_{pc} - T_s\right) + c_{l,pc} & T_m < T_{pc} \le T_l \\ c_{l,pc} & T_{pc} > T_l \end{cases} \tag{23}$$

In addition, the primary PCM density is the most crucial rheological characteristic to determine, especially throughout the phase transition. Thus, as indicated in Eq. (24), Maxwell [40] calculated the density by combining the solid and liquid phase densities. Besides, throughout the phase transition procedure, the thermal conductivity of base PCM is treated as a mixture of the thermal conductivities of solid and liquid phases Eq. (25). This correlation is developed by Vajjha and Das [41].

$$\rho_{pc} = \begin{cases} \rho_{pc,s} & T_{pc} \le T_s \\ lf\,.\,\rho_{pc,l} + \left(1 - lf\right)\rho_{pc,s} & T_s < T_{pc} \le T_m \\ \rho_{pc,l} & T_{pc} > T_l \end{cases} \tag{24}$$

$$k_{pc} = \begin{cases} k_{pc,s} & T_{pc} \leq T_s \\ lf \,.\, k_{pc,s} + \left(1 - lf\right) k_{pc,s} & T_s < T_{pc} \leq T_m \\ k_{pc,l} & T_{pc} > T_l \end{cases} \tag{25}$$

While lf referring to the liquid fraction of the PCM evaluated as (Eq. (26)):

$$lf = \left(T_{pc} - T_{pc,s}\right) / \left(T_{pc,l} - T_{pc,s}\right) \tag{26}$$

g. Working fluid

For the fluid, Eq. (27) has also been established.

$$m_f c_f \left(\frac{\partial T}{\partial t}\right)_f = h_{cv,\mathrm{f}-pc} A.(T_{pc} - T_f) - \left(\frac{\dot{m}}{n}\right)_f .c_f \left(\frac{\partial T}{\partial Y}\right)_f \Delta Y \tag{27}$$

While A and m_f denote the cooling tube's cross-sectional area and the fluid mass flow rate, respectively. Furthermore, the coefficient of heat exchange of the walls tube and the flowing water is expressed using the Bejan formula [42]. In addition, the Nusselt number was estimated according to Eq. (28), suggested by Duffie *et al.,* [35], which is valuable in the range of $1 < Re_f .Pr_f .d_{in} / L < 1000$.

$$Nu_f = 4.4 + \frac{0.00398.[\mathrm{Re}_f .\mathrm{Pr}_f .(d_{in} / L)]^{1.66}}{1 + 0.0114.[\mathrm{Re}_f .\mathrm{Pr}_f .(d_{in} / L)]^{1.12}} \tag{28}$$

h. Insulation

The insulation has constant thermophysical characteristics, and the investigation demonstrates heat transmission via convection between the insulation and the ambient, radiation, and convection with the cooling system. Additionally, Eq. (29) is employed to evaluate the equivalent coefficient heat transfer on the outer face of the insulation.

$$\rho_i c_i \delta_i \frac{\partial T_i}{\partial t} = h_{cd,i-pc} (\mathrm{T}_{pc} - \mathrm{T}_i) + h_{cv,i-\mathrm{am}} (\mathrm{T}_{am} - \mathrm{T}_i) \tag{29}$$

Here, $h_{cv,i-am}$ and $h_{cd,i-pc}$ denote the heat transfer coefficient by convection (Eq. (30)) and the heat transfer coefficient by conduction (Eq. (31)), respectively.

$$h_{cv,i-am} = \frac{\sigma \varepsilon_g (T_i^4 + T_{sky}^4)}{T_i - T_{am}} + \frac{Nu_{am} \lambda_{am}}{\delta} \tag{30}$$

$$h_{cd,i-pc} = \frac{\lambda_i}{\delta_i} \tag{31}$$

Table 1
Parameters of the various hybrid solar panel layers used in this work.

Layer	Parameter	Value [Refs]	
Glass cover	Emissivity	0.88 [33]	
	Specific heat ($J.kg^{-1}.K^{-1}$)	670 [33]	
	Density ($kg.m^{-3}$)	2500 [33]	
	Thickness (m)	0.0038 [33]	
PV plate	Packing factor	0.80 [27]	
	Temperature coefficient ($°C^{-1}$)	0.005 [27]	
	Reference cell efficiency η_{ref}	20% [27]	
	Thickness (m)	0.0003 [27]	
	Absorption coefficient	0.90 [27]	
Absorber plate (copper)	Thermal conductivity ($W.m^{-1}\ K^{-1}$)	400 [43]	
	Density ($kg.m^{-3}$)	8933 [43]	
	Thickness (m)	0.002 [43]	
	Specific heat ($J.kg^{-1}.K^{-1}$)	385 [43]	
		RT30	RT35
PCM (RT30 and RT35)	Thermal conductivity ($W.m^{-1}\ K^{-1}$)	0.2 [13]	0.2 [44]
	Thickness (m)	0.04 [13]	0.04 [44]
	Density ($kg.m^{-3}$): solid $\rho_{s,pc}$	870 [13]	800 [44]
	Liquid $\rho_{l,pc}$	760 [13]	800 [44]
	$T = T_s\ (°C)$ Solid phase	28 [13]	29 [44]
	$T_m = (T_s + T_l)/2\ (°C)$ Melting point	28.5 [13]	32.5 [44]
	$T_l\ (°C)$ Liquid phase	29 [13]	36 [44]
	Heat of fusion $Lh_{pc}\ \left(kJ\cdot kg^{-1}\right)$	222 [13]	130 [44]
	Specific Heat $\left(J.kg^{-1}.K^{-1}\right)$: solid $c_{s,pc}$	2400 [13]	2000 [44]
	Liquid $c_{l,pc}$	1800 [13]	2000 [44]
Insulation	Thermal conductivity ($W.m^{-1}\ K^{-1}$)	0.035 [33]	
	Density ($kg.m^{-3}$)	70 [33]	
	Thickness (m)	0.05 [33]	

3. Results and Discussion

3.1 Model Validation

3.1.1 Validation of the thermal model

To ensure its correctness, the created mathematical model was validated by comparing the forecast temperature findings as a proportion of daylight savings and the results obtained by Faddouli *et al.,* [33]. The contrast was carried out using the exact traditional PV panel specifications, bringing with consideration irradiation of 779 W/m^2, a surrounding temperature of 18 °C, an average wind velocity of 3mph, and a fluid flow rate of 0.01576 kg/s as reported by the authors.

According to Figure 2, the results of our modeling and the simulation by Faddouli *et al.,* [33] showed the highest accord. Notably, the maximum divergence is less than 1.5 °C in temperatures, leading to a maximum relative error of 0.5 %, which is highly acceptable. The results obtained in Figure 2 confirm the developed precision code to be employed in modeling PV and PV/T systems.

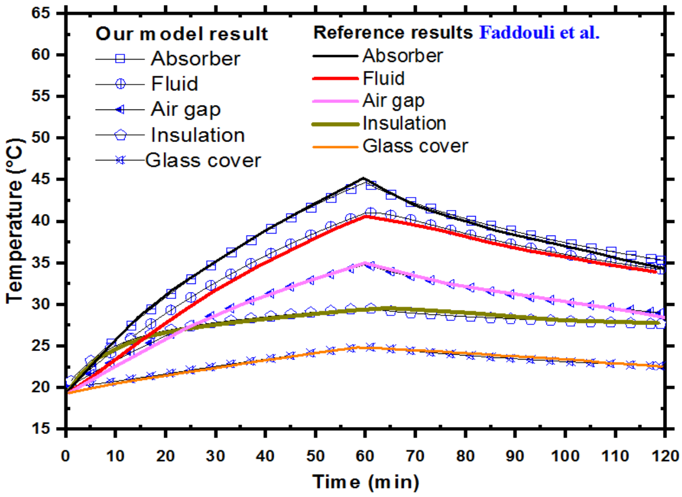

Fig. 2. The expected temperatures compared with that achieved by Faddouli *et al.,* [33]

3.1.2 Validation of the PV-PCM model

Abdelrazik *et al.,* [27] and Ma *et al.,* [45] studied the general effectiveness of a PV-PCM system. To make the model proposed for this work simple and adaptable to those of Abdelrazik *et al.,* [27] and Ma *et al.,* [45], the tubes and fluid circulation were eliminated. They investigated the system's performance at an ambient temperature of 35 °C, sunlight of 1000 W/m^2, and a wind speed of 0 m/s using the paraffin wax-RT35 characteristics listed in Table 1. The temperature Changes of the photovoltaic cells versus time in the simulation software used in the present work were contrasted to those of Abdelrazik *et al.,* [27] and Ma *et al.,* [45], revealing excellent agreement with an error rate of less than 2% as shown in Figure 3.

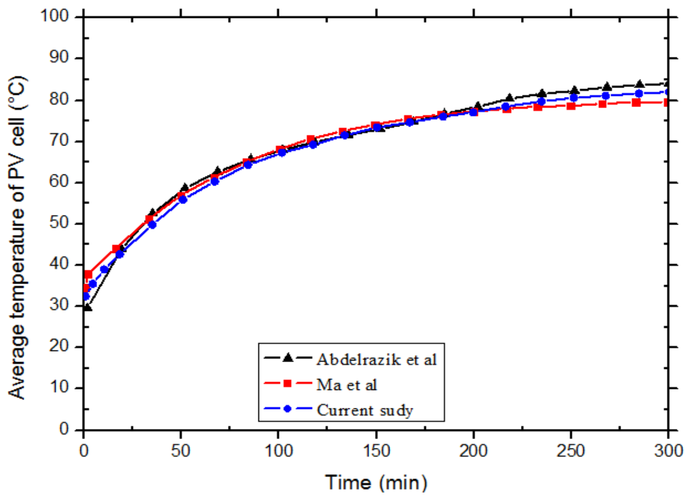

Fig. 3. Validation of the findings by comparing with those achieved by Abdelrazik *et al.,* [27] and Ma *et al.,* [45]

3.2 Meteorological Conditions

As illustrated in Figure 4, the surrounding temperature, solar radiation distributions, relativity humidity, and wind velocity in Ouarzazate city (Morocco) are taken for two days on the 4th of August

2022 (summer) and the other on the 4th of January 2023 (winter). The measures were taken at 1-minute time steps.

The ambient temperature ranged from 2.1°C and 20.5°C to 21.8 °C and 38.7°C in January and August, respectively (see Figure 4(a)). The temperature of the solar panels increases as the temperature of the surroundings rises, as indicated in (Eq. (11)) as shown in the same equation. According to the findings of Abdelrazik *et al.,* [27], the surrounding temperature lowers the cell temperature by acting as a natural cooling agent. Enhancing the irradiation results in a rise in the solar panel's temperature. The highest esteem of irradiation was 932.10 W/m2 and 1014.17 W/m^2 for January and August, respectively (see Figure 4(b), as Islam *et al.,* [46] reported that the increase in solar radiation leads to an improvement in the electrical efficiency of solar panels. Indeed, it is found that the humidity values decrease during the day. The minimum values are 13.9% and 3.8% in January and August, respectively (see Figure 4(c)), which is attributed to the inverse proportionality between the humidity and ambient temperature; a reduction in humidity causes a rise in PV panel temperature. The humidity reduction caused an improvement in the electrical power of solar panels, according to the results of Kazem and Chaichan [47]. This could be attributed to the higher solar irradiation received at the PV panels in cases of low moisture content.

Furthermore, the maximum wind speeds registered during the two days of the measurements were 3.6 m/s and 4.64 m/s, respectively (see Figure 4(d)). The higher wind speed decreases the modules' temperature for the investigated duration, as illustrated in Figure 10. The wind acts as a natural cooling agent, removing dust and thus lowering the cell temperature, according to the results of Ahmed *et al.,* [48].

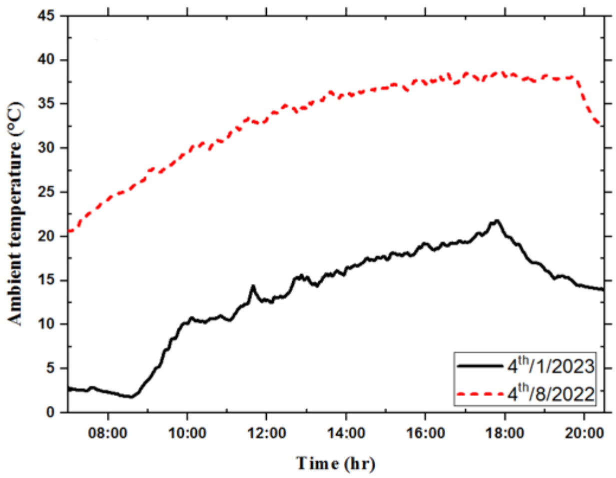

(a)

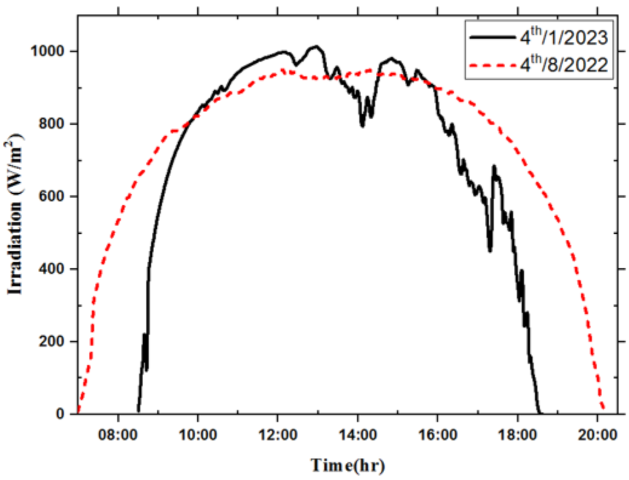

(b)

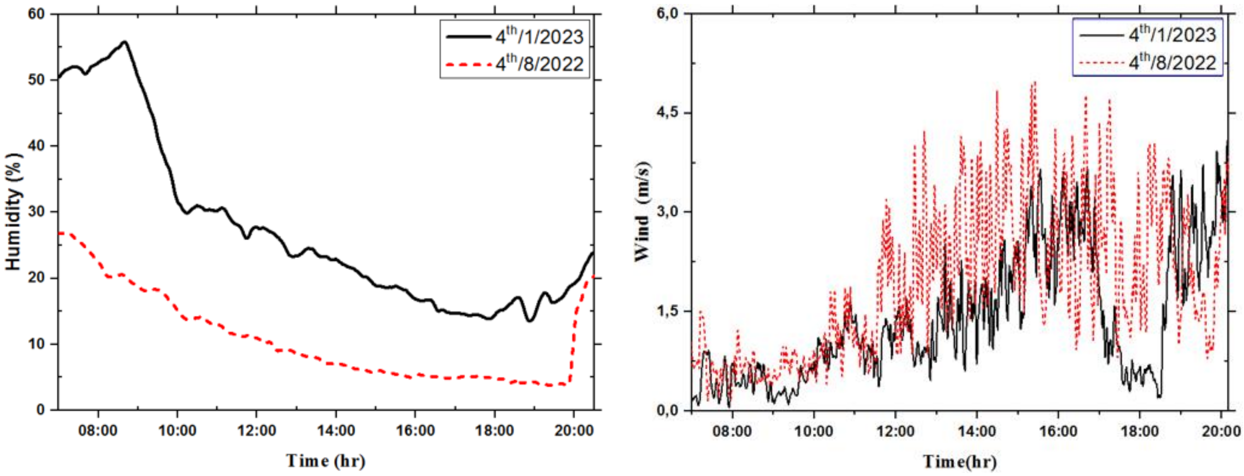

(c) (d)

Fig. 4. Measured meteorological conditions (the 4th of August, 2022, and the 4th of January, 2023) in Ouarzazat city: (a) ambient temperature, (b) solar irradiation, (c) relativity humidity, (d) wind speed

3.3 Photovoltaic Cells Temperature

Figure 5 presents the average PV cell temperature for PV/T, PV/T-PCM, and conventional PV systems versus solar time. Furthermore, attaching the PCM layer to the absorber plate, as well as using the water circulating in the pipe as a heat shield for the PV, significantly reduced its temperature in comparison to a standard PV device because of its significant latent heat storage compared to sensible heat storage, the PCM decreases the PV temperature and holds it at reduced temperatures before completely melting. In addition, as compared to other modules, the PV temperature in the PV/T-PCM has a gentler slope of temperature rise for the same time intervals. So when a system achieves its high temperature, the usage of PCMs maintains it at a reduced temperature and provides improved performance with hybrid systems during bright sunshine hours, which is one of the primary benefits of employing PCMs as heat sinks. The two days were chosen to depict efficiency in the summer and winter.

For the PV, PV/T, and PV/T-PCM systems, it was observed that the temperature of PV cells measured in August ranged from 20°C to 83.4 °C, 20°C to 72.5°C, and 20°C to 61.5°C, respectively, as indicated in Figure 5(a). The highest temperature decrease between PV and PV/T systems was approximately 11 °C (13.2%), and ~21.9 °C (26.25%) between PV and PV/T-PCM systems. It was found that the decrease in the PV temperature for the PV/T-PCM system compared to the PV/T panel started at 11:30 PM when the PV temperature exceeded 27.5°C, representing the melting point of RT30. Similar results were recently disclosed by Abdelrazik *et al.,* [27], where the PV/T and PV/T-PCM were studied. They detected that the PV/T-PCM module diminished the maximum temperature of PV cells by approximately 17°C compared to the standalone PV panel with the meteorological conditions of Dhahran City, Saudi Arabia.

However, the temperature of PV cells predicted in January for PV, PV/T, and PV/T-PCM modules ranged from 0°C to 65 °C, 0°C to 57 °C, and 0°C to 46 °C, respectively. It was found that the reduction in the PV temperature for the PV/T-PCM system, compared to the PV/T module, started at 9:30 PM when the PV temperature exceeded 27.5°C, representing the melting point of RT30. In this case, as displayed in Figure 5(b), the highest temperature reduction between PV and PV/T and PV and PV/T-PCM systems is approximately 12 °C (18.46%) and 19 °C (29.2%), respectively.

The concept behind incorporating a PCM part into a monocrystalline photovoltaic system is that PVs perform better at lower cell temperatures. In a PV-PCM, the PCM layer absorbs non-converted incidental solar radiation to electrical power with the photovoltaic cells, and it liquefies, leaving the PV panels cold and much more powerful.

The PV/T-PCM system is more recommended than the PV/T and PV systems for decreasing the solar panel's temperature; this lower temperature makes it possible to improve the electrical yield, as seen in the following section.

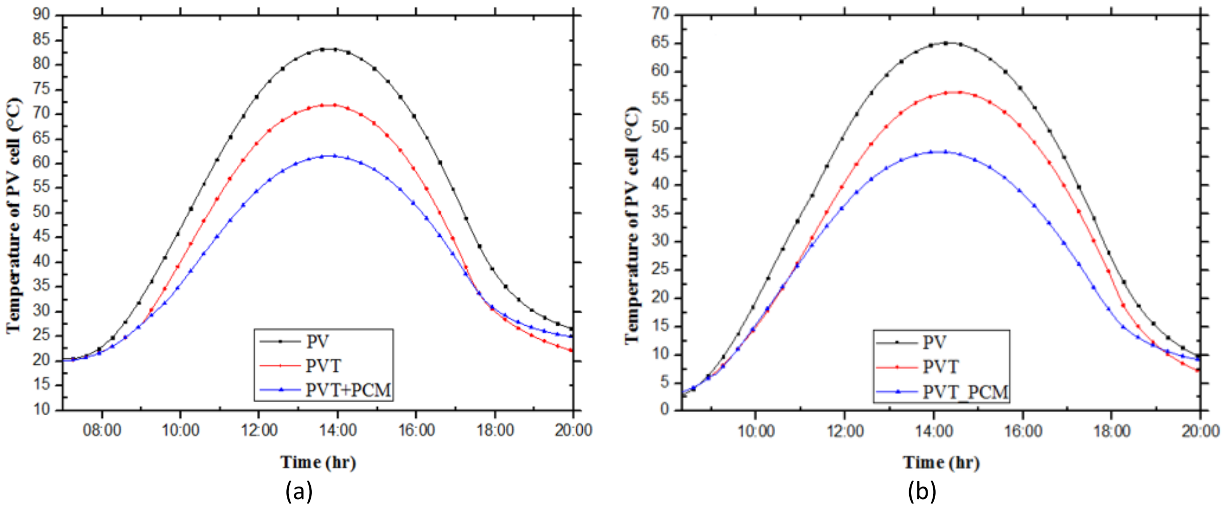

Fig. 5. Variation in the PV panel's temperature over time in different systems during (a) the 4th of August, 2022 and (b) the 4th of January, 2023

3.4 Electrical Efficiency

In this subsection, the distribution of the electrical efficiency over time for PV/T, PV/T-PCM, and PV modules is depicted in Figure 6. The results declared that at higher PV temperatures, the PV electrical efficiency decreases. This conduct is evident so that as the PV temperature rises, the power generated tends to reduce, as shown in the efficiency formula (Eq. (16)). For the fourths of January and August versus the conventional photovoltaic panel, the maximum PV efficiency increases in the PV/T were around 0.8% and 1%, respectively. The PV/T-PCM is relatively more efficient in increasing electrical performance in January than in August, as shown in Figure 6, because of the relatively high level of sunlight intensity in the midday on the 4th of January, compared to the same time of day in August. Attaching a PCM sheet as a heat sink decreased the PV temperature in the PV/T-PCM during the peak sun hour as described in Section "Photovoltaic cells temperature", enhancing PV efficiency compared to a solo PV. The maximum increases on the 4th of August and the 4th of January were 1.95 % and 1.65 %, respectively. A similar result was indicated by Abdelrazik *et al.,* [27]. They have reported an improved electrical efficiency of the PV/T-PCM module by about 1.7 % compared to the traditional PV panel in mid-July in Dhahran City, Saudi Arabia.

The comparison between the daylight simulation on the 4^{th} of August and the 4^{th} of January 4^{th} revealed that the efficiency-increasing effect of the PV/T-PCM model was noticeable in the summer compared to the traditional PV, which was attributed to the high solar radiation intensity throughout the day on the 4^{th} of August compared to the same day in January (see Figure 6). The findings reveal that the thermal control impacts of PCM and PV/T are fundamentally different, with PCM causing a time shift in temperature increase. At the same time, PV/T-PCM lowers the maximum temperature, increasing the electrical efficiency.

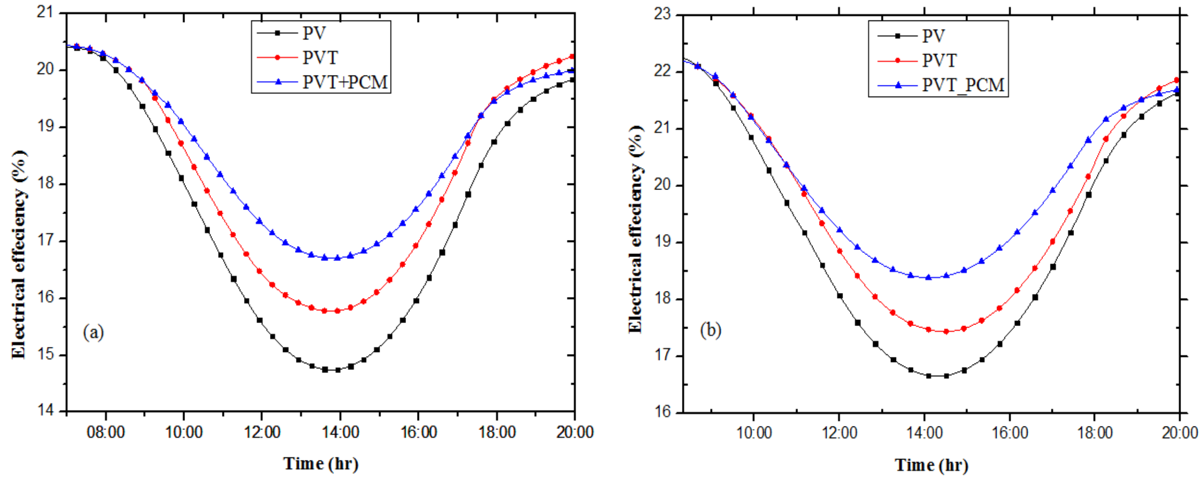

(a) (b)

Fig. 6. Fluctuation in the PV panel's electrical efficiency over time for different systems during the 4th of August, 2022 (a), and the 4th of January, 2023 (b)

3.5 The PCM Thickness Impact

The impact of PCM layer thickness on PV temperature variation has been studied using the numerical model. The surrounding temperature is considered constant at 25°C, and the solar irradiation is supposed to be 800 W/m^2. The highest PV cell temperatures achieved for thicknesses of 50 mm, 40 mm, 30 mm, 20 mm, 10 mm are 47.4 °C, ~ 47.4 °C, 48.5 °C, 49.9 °C, and 52.2 °C respectively as shown in Figure 7.

This temperature reduction is caused by the corresponding correlation between the PCM's thickness and its overall volume. Moreover, the best thicknesses of phase change material that give significant temperature drops are 40 mm and 50 mm. Afterward, the solar panel's temperature slowly rises. The greater the volume of the PCM, the more time it needs to melt completely. However, due to low PCM thermal conductivity, increasing the layer thickness decreases resistance to heat rejection from the rear of the PV panel, causing a decrease in the panel's temperature. Besides, the panel's response time to reach a maximum temperature increases with the thickness of the PCM layer. These results match with those provided by Bria *et al.,* [49] and Maghrabie *et al.,* [50] as they reported that the increase of the layer thickness of the PCM decreased the temperature of the PV/PCM hybrid system.

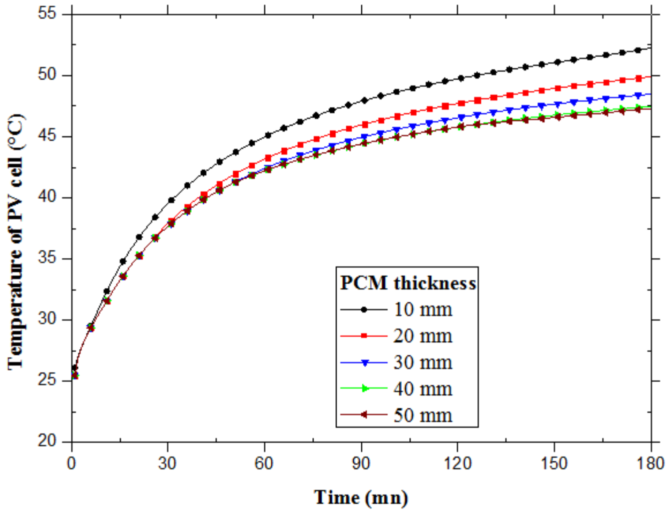

Fig. 7. The impact of PCM layer thickness on PV temperature compared to a conventional PV module without PCM

3.6 The Ambient Temperature Impact

Figure 8 depicts the effect of different atmospheric temperatures on the PV temperature distribution at the irradiation constant of 800 W/m^2 and wind speed constant of 1 m/s. The variation in temperature shows higher rises in PV temperature at increased surrounding temperatures. The temperature of the solar panels increases as the ambient temperature rises, as expressed in Eq. (11). The ambient temperature acts as a natural cooling agent and lowers the cell temperature, according to the results of Abdelrazik *et al.,* [27].

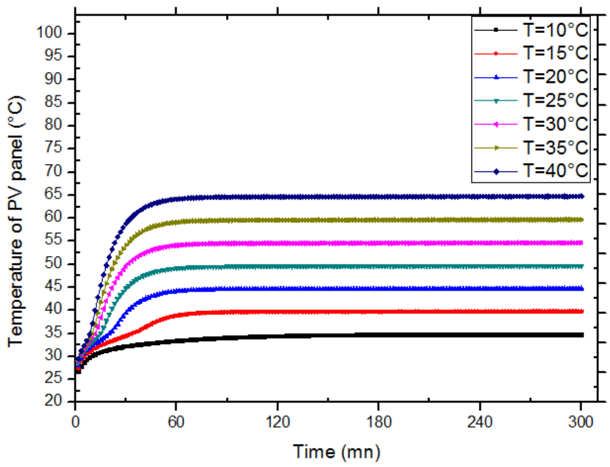

Fig. 8. The impact of the ambient temperature on the PV panel temperature in the PV/T-PCM system

3.7 The Irradiation Impact

At 25°C and 1 m/s for ambient temperature and wind speed, respectively, the temperature of the PV/T-PCM module was conducted at different irradiation intensities. The finding illustrated that the PV temperature distribution is increased at higher irradiation, as shown in Figure 9. According to the results of Dubey *et al.,* [51], the wind acts as a natural cooling agent, removing dust and thus lowering the cell temperature.

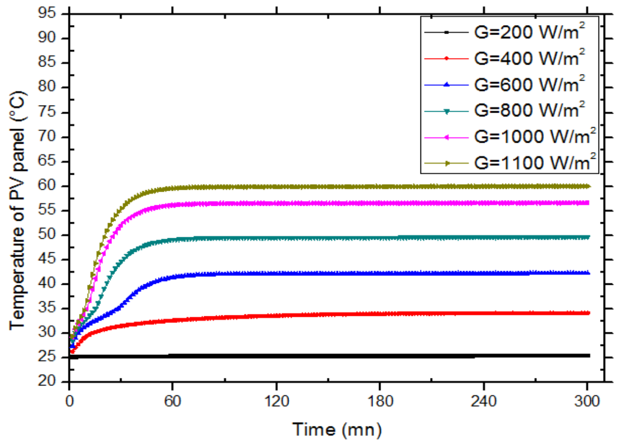

Fig. 9. The effect of irradiation on the PV panel temperature in the PV/T-PCM system

3.8 The Wind Speed Impact

Figure 10 illustrates the effect of different wind speed on the PV temperature distribution at the irradiation constant of 800 W/m^2 and ambient temperature constant of 25°C. The distribution of temperatures shows that the rate of rise in PV temperature is more elevated at lower wind speeds. The wind reflects an advantageous impact on solar panels by cooling them with raised convection. According to Ahmed *et al.,* [48], the wind acts as a natural cooling agent, removing dust and thus lowering the cell temperature.

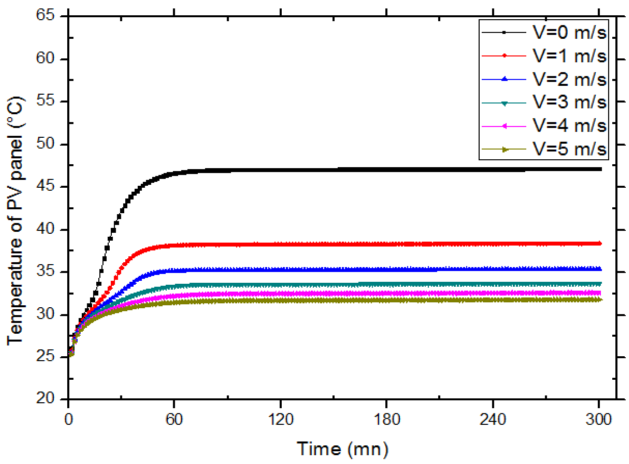

Fig. 10. The effect of the wind speed on the PV panel temperature in the PV/T-PCM system

4. Conclusions

In this research, the electrical performances of PV/T-PCM, PV/T, and PV systems were evaluated and compared by developing three different models for the three systems and by employing the Finite Difference Method (FDM) to the governing energy equations. The simulations were conducted to model the transient energy conversion processes in all of the PV/T-PCM, PV/T, and PV modules. The simulations have been carried out using actual meteorological conditions over two days in Ouarzazate, Morocco (the 4th of August, 2022, and the 4th of January, 2023). The findings concerning the 4th of January, 2023, indicate that PV/T-PCM is discovered to decrease the temperature of PV cells to nearly 19 °C (29.2%), consequently increasing their electrical efficiency by 1.65 %. Additionally, the PV/T diminishes the photovoltaic cell's temperature by approximately 12°C (18.46%). Consequently, the electrical efficiency rises by 0.8 % compared to the conventional PV system. On the 4th of August, 2022, it is revealed that the PV/T-PCM reduces the temperature of PV cells by approximately 21.9° (26.25%) compared to the traditional photovoltaic panel. Therefore, the electrical efficiency increases by 1.95%. Moreover, it is discovered that the PV/T decreases the temperature of the PV layer by about 11 °C (13.2%), which consequently increases the electrical efficiency by 1%.

Combining PCM with hybrid PV/T-based systems is a good solution for lowering PV temperature and improving system electrical performance. Larger PCM thicknesses, on the other hand, are not recommended.

These interesting PV/T and PV/T-PCM systems are advantageous for industrial applications because they can effectively contribute to meeting both electricity and thermal needs and significantly cover industrial thermal loads.

PV/T-PCM temperature decreases noticeably when solar radiation intensity and ambient temperature decrease while wind speed increases. For the application of this method of cooling solar panels, it is recommended that phase-change material be integrated with the PV/T system to significantly improve the electrical efficiency of solar panels.

Lastly, this study represents the starting point for the evaluation of PV/T-PCM, PV/T, and PV systems. The nanoPCM layer will be taken into account for the actual modes. The thermo physical characteristics of the PCM layer will be improved; cooling will be efficient and increase the PV electrical efficiency.

Authors' Contributions

Mohamed Bouzelmad: Conceptualization, Software, Visualization, Investigation, Methodology, Writing – original draft. **Youssef Belkassmi**: Supervision, Conceptualization, Writing – review & editing, Methodology, Validation, Resources. **Ahmed Abdelrazik**: Supervision, Conceptualization, Writing – review & editing, Methodology, Validation, Resources. **Abdelhadi Kotri**: Supervision, Conceptualization, Writing – review & editing, Methodology, Validation, Resources. **Mohamed Gounzari**: Conceptualization, Software, Visualization, Investigation, Methodology, Writing . **Mustapha Sahal:** Conceptualization , Writing – review & editing, Visualization.

Acknowledgments
The authors gratefully acknowledge the HPC-MARWAN (www.marwan.ma/hpc) software resources supplied by the Centre National de la Recherche Scientifique et Technique (CNRST), Rabat, Morocco.

Conflict of Interest
The authors declare that they have no conflict of interest.

Data Availability
The research data of this manuscript will not be available.

References
[1] Wang, Qing, Chunlei Wu, Xinmin Wang, Shipeng Sun, Da Cui, Shuo Pan, and Hongyu Sheng. "A review of eutectic salts as phase change energy storage materials in the context of concentrated solar power." *International Journal of Heat and Mass Transfer* 205 (2023): 123904. https://doi.org/10.1016/j.ijheatmasstransfer.2023.123904
[2] Xu, Yanyan, Yanqin Xue, Weihua Cai, Hong Qi, and Qian Li. "Experimental study on performances of flat-plate

pulsating heat pipes coupled with thermoelectric generators for power generation." *International Journal of Heat and Mass Transfer* 203 (2023): 123784. https://doi.org/10.1016/j.ijheatmasstransfer.2022.123784

[3] Islam, M. M., A. K. Pandey, M. Hasanuzzaman, and N. A. Rahim. "Recent progresses and achievements in photovoltaic-phase change material technology: A review with special treatment on photovoltaic thermal-phase change material systems." *Energy Conversion and Management* 126 (2016): 177-204. https://doi.org/10.1016/j.enconman.2016.07.075

[4] Rejeb, Oussama, Houcine Dhaou, and Abdelmajid Jemni. "A numerical investigation of a photovoltaic thermal (PV/T) collector." *Renewable Energy* 77 (2015): 43-50. https://doi.org/10.1016/j.renene.2014.12.012

[5] Bouzelmad, Mohamed, Youssef Belkassmi, Abdelhadi Kotri, Lahoucine Elmaimouni, Mohammed Gounzari, and Abdelaziz Benahmida. "Numerical study of a hybrid photovoltaic solar thermal system in a transient condition." In *2021 9th International Renewable and Sustainable Energy Conference (IRSEC)*, pp. 1-6. IEEE, 2021. https://doi.org/10.1109/IRSEC53969.2021.9741182

[6] Maiti, Subarna, Sudhanya Banerjee, Kairavi Vyas, Pankaj Patel, and Pushpito K. Ghosh. "Self regulation of photovoltaic module temperature in V-trough using a metal-wax composite phase change matrix." *Solar Energy* 85, no. 9 (2011): 1805-1816. https://doi.org/10.1016/j.solener.2011.04.021

[7] Reddy, Sohail R., Mohammad A. Ebadian, and Cheng-Xian Lin. "A review of PV-T systems: Thermal management and efficiency with single phase cooling." *International Journal of Heat and Mass Transfer* 91 (2015): 861-871. https://doi.org/10.1016/j.ijheatmasstransfer.2015.07.134

[8] Abdullah, Amira Lateef, Suhaimi Misha, Noreffendy Tamaldin, Mohd Afzanizam Mohd Rosli, and Fadhil Abdulameer Sachit. "Hybrid photovoltaic thermal PVT solar systems simulation via Simulink/Matlab." *CFD Letters* 11, no. 4 (2019): 64-78.

[9] Sachit, Fadhil Abdulameer, Mohd Afzanizam Mohd Rosli, Noreffendy Tamaldin, Suhaimi Misha, and Amira Lateef Abdullah. "Modelling, validation and analyzing performance of serpentine-direct PV/T solar collector design." *CFD Letters* 11, no. 2 (2019): 50-65.

[10] Płaczek-Popko, E. "Top PV market solar cells 2016." *Opto-Electronics Review* 25, no. 2 (2017): 55-64. https://doi.org/10.1016/j.opelre.2017.03.002

[11] Feldman, David, K. Wu, and R. Margolis. "Solar industry update." *National Renewable Energy laboratory (NREL)* (2021). https://doi.org/10.2172/1808491

[12] Elarga, Hagar, Francesco Goia, Angelo Zarrella, Andrea Dal Monte, and Ernesto Benini. "Thermal and electrical performance of an integrated PV-PCM system in double skin façades: A numerical study." *Solar Energy* 136 (2016): 112-124. https://doi.org/10.1016/j.solener.2016.06.074

[13] Preet, Sajan, Brij Bhushan, and Tarun Mahajan. "Experimental investigation of water based photovoltaic/thermal (PV/T) system with and without phase change material (PCM)." *Solar Energy* 155 (2017): 1104-1120. https://doi.org/10.1016/j.solener.2017.07.040

[14] Ramakrishnan, Sayanthan, Xiaoming Wang, and Jay Sanjayan. "Effects of various carbon additives on the thermal storage performance of form-stable PCM integrated cementitious composites." *Applied Thermal Engineering* 148 (2019): 491-501. https://doi.org/10.1016/j.applthermaleng.2018.11.025

[15] Kılkış, Birol. "Development of a composite PVT panel with PCM embodiment, TEG modules, flat-plate solar collector, and thermally pulsing heat pipes." *Solar Energy* 200 (2020): 89-107. https://doi.org/10.1016/j.solener.2019.10.075

[16] Hossain, M. S., A. K. Pandey, Jeyraj Selvaraj, Nasrudin Abd Rahim, M. M. Islam, and V. V. Tyagi. "Two side serpentine flow based photovoltaic-thermal-phase change materials (PVT-PCM) system: Energy, exergy and economic analysis." *Renewable Energy* 136 (2019): 1320-1336. https://doi.org/10.1016/j.renene.2018.10.097

[17] Rosli, Mohd Afzanizam Mohd, Nurfarhana Salimen, Nurul Izzati Akmal Muhamed Rafaizul, Suhaimi Misha, Norli Abdullah, Safarudin Gazali Herawan, Avita Ayu Permanasari, and Faridah Hussain. "Parametric Study of Photovoltaic System Integrated with Organic Phase Change Material using ANSYS." *Journal of Advanced Research in Fluid Mechanics and Thermal Sciences* 106, no. 1 (2023): 76-89. https://doi.org/10.37934/arfmts.106.1.7689

[18] Hindi, Noor Abbas, Saadoon Fahad Dakhil, and Karrar Abdullah Abbas. "Experimental Study to Improve Solar Photovoltaic Performance by Utilizing PCM and Finned Wall." *Journal of Advanced Research in Fluid Mechanics and Thermal Sciences* 102, no. 1 (2023): 153-170. https://doi.org/10.37934/arfmts.102.1.153170

[19] Atkin, Peter, and Mohammed M. Farid. "Improving the efficiency of photovoltaic cells using PCM infused graphite and aluminium fins." *Solar Energy* 114 (2015): 217-228. https://doi.org/10.1016/j.solener.2015.01.037

[20] Farid, Mohammed M., Amar M. Khudhair, Siddique Ali K. Razack, and Said Al-Hallaj. "A review on phase change energy storage: materials and applications." *Energy Conversion and Management* 45, no. 9-10 (2004): 1597-1615. https://doi.org/10.1016/j.enconman.2003.09.015

[21] Hasan, Ahmed, S. J. McCormack, M. J. Huang, and Brian Norton. "Evaluation of phase change materials for thermal regulation enhancement of building integrated photovoltaics." *Solar Energy* 84, no. 9 (2010): 1601-1612.

https://doi.org/10.1016/j.solener.2010.06.010

[22] Hussain, F., M. Y. H. Othman, B. Yatim, H. Ruslan, K. Sopian, and Z. Ibarahim. "A study of PV/T collector with honeycomb heat exchanger." In *AIP Conference Proceedings*, vol. 1571, no. 1, pp. 10-16. American Institute of Physics, 2013. https://doi.org/10.1063/1.4858622

[23] Park, Jungwoo, Taeyeon Kim, and Seung-Bok Leigh. "Application of a phase-change material to improve the electrical performance of vertical-building-added photovoltaics considering the annual weather conditions." *Solar Energy* 105 (2014): 561-574. https://doi.org/10.1016/j.solener.2014.04.020

[24] Fudholi, Ahmad, Kamaruzzaman Sopian, Mohammad H. Yazdi, Mohd Hafidz Ruslan, Adnan Ibrahim, and Hussein A. Kazem. "Performance analysis of photovoltaic thermal (PVT) water collectors." *Energy Conversion and Management* 78 (2014): 641-651. https://doi.org/10.1016/j.enconman.2013.11.017

[25] Hou, Longshu, Zhenhua Quan, Yaohua Zhao, Lincheng Wang, and Gang Wang. "An experimental and simulative study on a novel photovoltaic-thermal collector with micro heat pipe array (MHPA-PV/T)." *Energy and Buildings* 124 (2016): 60-69. https://doi.org/10.1016/j.enbuild.2016.03.056

[26] Huo, Yuxia, Jian Lv, Xianli Li, Lishuo Fang, Xuejian Ma, and Qi Shi. "Experimental study on the tube plate PV/T system with iron filings filled." *Solar Energy* 185 (2019): 189-198. https://doi.org/10.1016/j.solener.2019.04.041

[27] Abdelrazik, A. S., F. A. Al-Sulaiman, and R. Saidur. "Numerical investigation of the effects of the nano-enhanced phase change materials on the thermal and electrical performance of hybrid PV/thermal systems." *Energy Conversion and Management* 205 (2020): 112449. https://doi.org/10.1016/j.enconman.2019.112449

[28] Belkassmi, Youssef, Kamal Gueraoui, Lahoucine El maimouni, Najem Hassanain, and Omar Tata. "Numerical Investigation and Optimization of a Flat Plate Solar Collector Operating with Cu/CuO/Al_2O_3-Water Nanofluids." *Transactions of Tianjin University* 27 (2021): 64-76. https://doi.org/10.1007/s12209-020-00272-6

[29] Samylingam, L., Navid Aslfattahi, R. Saidur, Syed Mohd Yahya, Asif Afzal, A. Arifutzzaman, K. H. Tan, and K. Kadirgama. "Thermal and energy performance improvement of hybrid PV/T system by using olein palm oil with MXene as a new class of heat transfer fluid." *Solar Energy Materials and Solar Cells* 218 (2020): 110754. https://doi.org/10.1016/j.solmat.2020.110754

[30] Das, Dudul, Urbashi Bordoloi, Akash Dilip Kamble, Harrison Hihu Muigai, Ranjith Krishna Pai, and Pankaj Kalita. "Performance investigation of a rectangular spiral flow PV/T collector with a novel form-stable composite material." *Applied Thermal Engineering* 182 (2021): 116035. https://doi.org/10.1016/j.applthermaleng.2020.116035

[31] Ke, Wei, Jie Ji, Lijie Xu, Bendong Yu, Xinyi Tian, and Jun Wang. "Numerical study and experimental validation of a multi-functional dual-air-channel solar wall system with PCM." *Energy* 227 (2021): 120434. https://doi.org/10.1016/j.energy.2021.120434

[32] Abdelrazik, A. S., F. A. Al-Sulaiman, and R. Saidur. "Feasibility study for the integration of optical filtration and nano-enhanced phase change materials to the conventional PV-based solar systems." *Renewable Energy* 187 (2022): 463-483. https://doi.org/10.1016/j.renene.2022.01.095

[33] Faddouli, A., H. Labrim, S. Fadili, A. Habchi, B. Hartiti, M. Benaissa, M. Hajji, H. Ez-Zahraouy, E. Ntsoenzok, and A. Benyoussef. "Numerical analysis and performance investigation of new hybrid system integrating concentrated solar flat plate collector with a thermoelectric generator system." *Renewable Energy* 147 (2020): 2077-2090. https://doi.org/10.1016/j.renene.2019.09.130

[34] Swinbank, W. C. "Long-wave radiation from clear skies." *Quarterly Journal of the Royal Meteorological Society* 89, no. 381 (1963): 339-348. https://doi.org/10.1002/qj.49708938105

[35] Duffie, John A., William A. Beckman, and Jon McGowan. "Solar Engineering of Thermal Processes." *American Journal of Physics* 53, no. 4 (1985): 382-382. https://doi.org/10.1119/1.14178

[36] Hollands, K. G. T., T. E. Unny, G. D. Raithby, and L. Konicek. "Free convective heat transfer across inclined air layers." *ASME Journal of Heat and Mass Transfer* 98, no. 2 (1976): 189-193. https://doi.org/10.1115/1.3450517

[37] Kalogirou, Soteris A. *Solar Energy Engineering: Processes and Systems*. Academic Press, 2009.

[38] Zhou, Yuekuan, Xiaohong Liu, and Guoqiang Zhang. "Performance of buildings integrated with a photovoltaic-thermal collector and phase change materials." *Procedia Engineering* 205 (2017): 1337-1343. https://doi.org/10.1016/j.proeng.2017.10.109

[39] Bhattarai, Sujala, Jae-Heun Oh, Seung-Hee Euh, Gopi Krishna Kafle, and Dae Hyun Kim. "Simulation and model validation of sheet and tube type photovoltaic thermal solar system and conventional solar collecting system in transient states." *Solar Energy Materials and Solar Cells* 103 (2012): 184-193. https://doi.org/10.1016/j.solmat.2012.04.017

[40] Maxwell, James Clerk. *A treatise on electricity and magnetism*. Vol. 1. Clarendon press, 1873.

[41] Vajjha, Ravikanth S., and Debendra K. Das. "Experimental determination of thermal conductivity of three nanofluids and development of new correlations." *International Journal of Heat and Mass Transfer* 52, no. 21-22 (2009): 4675-4682. https://doi.org/10.1016/j.ijheatmasstransfer.2009.06.027

[42] Bejan, Adrian. "Constructal-theory network of conducting paths for cooling a heat generating volume." *International Journal of Heat and Mass Transfer* 40, no. 4 (1997): 799-816. https://doi.org/10.1016/0017-9310(96)00175-5
[43] Hissouf, Mohamed, Monssif Najim, and Adil Charef. "Effect of optical, geometrical and operating parameters on the performances of glazed and unglazed PV/T system." *Applied Thermal Engineering* 197 (2021): 117358. https://doi.org/10.1016/j.applthermaleng.2021.117358
[44] Ma, Tao, Zhenpeng Li, and Jiaxin Zhao. "Photovoltaic panel integrated with phase change materials (PV-PCM): technology overview and materials selection." *Renewable and Sustainable Energy Reviews* 116 (2019): 109406. https://doi.org/10.1016/j.rser.2019.109406
[45] Ma, Tao, Jiaxin Zhao, and Zhenpeng Li. "Mathematical modelling and sensitivity analysis of solar photovoltaic panel integrated with phase change material." *Applied Energy* 228 (2018): 1147-1158. https://doi.org/10.1016/j.apenergy.2018.06.145
[46] Islam, Md Nazrul, Mohammad Ziaur Rahman, and Sharif Mohammad Mominuzzaman. "The effect of irradiation on different parameters of monocrystalline photovoltaic solar cell." In *2014 3rd International Conference on the Developments in Renewable Energy Technology (ICDRET)*, pp. 1-6. IEEE, 2014. https://doi.org/10.1109/ICDRET.2014.6861716
[47] Kazem, Hussein A., and Miqdam T. Chaichan. "Effect of humidity on photovoltaic performance based on experimental study." *International Journal of Applied Engineering Research (IJAER)* 10, no. 23 (2015): 43572-43577.
[48] Ahmed, Md Shakil, Raihan Karal, Barun K. Das, and Arnob Das. "Experimental investigation of cooling, wind velocity, and dust deposition effects on solar PV performance in a tropical climate in Bangladesh." *Case Studies in Thermal Engineering* 50 (2023): 103409. https://doi.org/10.1016/j.csite.2023.103409
[49] Bria, Abir, Benyounes Raillani, Dounia Chaatouf, Mourad Salhi, Samir Amraqui, and Ahmed Mezrhab. "Effect of PCM Thickness on the Performance of the Finned PV/PCM System." *Materials Today: Proceedings* 72 (2023): 3617-3625. https://doi.org/10.1016/j.matpr.2022.08.409
[50] Maghrabie, Hussein M., A. S. A. Mohamed, Amany M. Fahmy, and Ahmed A. Abdel Samee. "Performance enhancement of PV panels using phase change material (PCM): An experimental implementation." *Case Studies in Thermal Engineering* 42 (2023): 102741. https://doi.org/10.1016/j.csite.2023.102741
[51] Dubey, Swapnil, Jatin Narotam Sarvaiya, and Bharath Seshadri. "Temperature dependent photovoltaic (PV) efficiency and its effect on PV production in the world-a review." *Energy Procedia* 33 (2013): 311-321. https://doi.org/10.1016/j.egypro.2013.05.072